Surface-enhanced Raman scattering studies on immunoassay

Shuping Xu
Jilin University
Key Laboratory for Supramolecular Structure
    and Material of Ministry of Education
Changchun 130012, People's Republic of China
    and
Kwansei-Gakuin University
Department of Chemistry
School of Science and Technology
Sanda, Hyogo 669-1337, Japan

Xiaohui Ji
Jilin University
College of Chemistry
Changchun 130021, People's Republic of China

Weiqing Xu
Bing Zhao
Jilin University
Key Laboratory for Supramolecular Structure
    and Material of Ministry of Education
Changchun 130012, People's Republic of China

Xiaoming Dou
Shanghai Jiao Tong University
Molecular and Photonics Laboratory
Physical Department
Shanghai 200030, People's Republic of China

Yubai Bai
Jilin University
College of Chemistry
Changchun 130021, People's Republic of China

Yukihiro Ozaki
Kwansei-Gakuin University
Department of Chemistry
School of Science and Technology
Sanda, Hyogo 669-1337, Japan

Abstract. Surface-enhanced Raman scattering (SERS) has recently been a matter of keen interest from the points of both basic science and applications because by using the SERS effect one can obtain Raman signals even from a single molecule. Immunoassay is one of the most promising fields in the applications of SERS, and the purpose of this review paper is to discuss the potential of SERS in immunoassay. This paper consists of four parts work on the indirect and direct methods of immunoassay via SERS. These methods provide the laboratorial attempts on biomedical diagnostic applications of SERS. © *2005 Society of Photo-Optical Instrumentation Engineers.* [DOI: 10.1117/1.1915487]

Introduction

For the last three decades Raman spectroscopy has been extensively employed to investigate biological molecules and materials, because it can provide rich structural information as well as quantitative and qualitative information about them, and moreover, it can be applied to aqueous samples and samples under physiological conditions in a nondestructive manner.[1–3] However, Raman spectroscopy has one serious disadvantage; the sensitivity of Raman spectroscopy is not enough for various biological or biomedical applications. Therefore, many trials have been made to improve or enhance the sensitivity of Raman spectroscopy. The use of resonance Raman effect is one of them. Recent marked progress in Raman instrumentation has improved largely the sensitivity of Raman spectroscopy. However, still the sensitivity of Raman spectroscopy is often insufficient particularly for the quantitative analysis, and microanalysis of biological molecules with the low concentration.

Surface-enhanced Raman scattering (SERS) has recently been a matter of keen interest because it can readily enhance Raman signals by a factor of 10^{3-14}.[4–10] Since the success of Raman measurements of single molecules by SERS,[11,12] SERS has attracted much greater attention than before from the points of both basic science and applications. Recent remarkable progress in the studies of the mechanism of SERS and its experimental techniques has broadened and strengthened the potential of Raman spectroscopy in the applications of biology and medicine.

SERS has three major advantages for bioanalytical applications.[13–20] One is the enormous enhancement of the Raman cross section of adsorbed molecules by a factor of $10^3 – 10^{14}$.[6–12] When SERS is applied to a quantitative assay,

Address all correspondence to Yukihiro Ozaki, Department of Chemistry, School of Science and Technology, Kwansei-Gakuin University, Sanda, Hyogo 669-1337 Japan. Tel: +81-79-565-8349; Fax: +81-79-565-9077; E-mail: ozaki@kwansei.ac.jp

one can achieve higher sensitivity and lower detection limit. The SERS effect becomes even more remarkable if the frequency of the excitation light is in resonance with a major absorption band of the adsorbed molecules being illuminated surface-enhance resonance Raman scattering (SERRS). Second, in SERS spectra there is a marked reduction in the fluorescence background that often interferes Raman scattering from biological molecules. The third advantage is the surface selectivity that the SERS effect provides. This means that only molecules or molecular segments on or very close to a metal surface can yield SERS signals.

Recently, a great number of SERS studies have been carried out by using noble metal colloid nanoparticles, which are small in size by comparison with the wavelength of the incident light. The shape and size of single metal nanoaggregates govern the overall enhancement.[21,22] SERS of molecules adsorbed on colloidal Ag and Ag nanoaggregates in a solution offers new and interesting possibilities as an analytical tool for detecting various types of molecules at extremely low concentrations.

SERS holds great possibility for the investigations of biological materials from small molecules to tissues. SERS-based bioanalytical applications include the following: (1) Microanalysis or trace analysis of simple biological compounds such as amino acids, nucleotides, and biological pigments.[23–36] Because of the very high sensitivity of SERS, one can obtain Raman spectra of biological molecules at concentrations down to $\sim 10^{-13}$ mol/L. (2) DNA gene probes, gene diagnosis, quantitative assay of double-stranded DNA, and studies of antitumor drug target complexes.[37–48] (3) Assay of thiol groups.[49] (4) Enzyme immunoassay employing SERS.[50–59] (5) The SERS microprobe approach in the determination of the distribution of biological species and drug within the living cell.[60–62]

Immunoassay, which is based on a specific interaction between an antigen and a complementary antibody, is a powerful analytical tool for biochemical analyses, clinical diagnosis, and environmental monitoring, and is one of the most promising fields in the applications of SERS. The purpose of this review paper is to discuss the potential of SERS in immunoassay. Many analysis methods, such as surface plasmon resonance,[63–66] atomic force microscopy[67–72] (AFM), and quartz crystal microbalance,[73,74] electrochemical detection,[75] have been developed for a direct measurement of the antigens binding to antibody molecules immobilized on a substrate. To increase the detection sensitivity of analytes, many kinds of conventional labelling immunoassay techniques, e.g., enzyme-linked immunosorbent assay[76,77] (ELISA), fluorescence,[78,79] and chemiluminescence,[80–83] have widely been applied. Recently, metallic colloid nanoparticles have also been successfully applied to the label techniques in immunoassay because of their easily controllable-size distribution, long-term stability, and friendly biocompatibility with antibodies, antigen proteins, DNA, and RNA.[84–94] Many novel methods using metallic colloid nanoparticles have been developed, such as colloidal Au labeling immunoassay systems detected with transmission electron microscopy[88] or scanning electron microscopy,[89] even by nakedeye,[90–93] imaging of gold colloidal particles by conjugating the immune complexes on conductive substrates with scanning tunneling microscope,[94] and so on.

Raman spectroscopy has been thought to hold considerable promise for enzyme immunoassay because, showing abundant, yet sharp and well-resolved bands, it contains much chemical information useful for enzyme immunoassay.[50–59] However, in general, the sensitivity of Raman spectroscopy is not enough for immunoassay. In order to overcome this difficulty, Cotton et al.[50] utilized SERRS effect for Raman enzyme immunoassay. In their system, resonance dye, p-dimethylaminoazobenzene was covalently attached to an antibody directed against human thyroid simulating hormone (TSH), and the resultant conjugate was used as the reported molecule in a sandwich immunoassay for TSH antigen. The intensity of the resultant SERRS signals showed a good correlation with TSH antigen concentration over a range of from 4 to 60 μIU/mL[50] (equal to about 10^{-6} mg/mL).

The SERS method has several advantages for enzyme immunoassay over other spectroscopic techniques. First, a SERS spectrum shows very specific and narrow Raman lines, minimizing the spectroscopic overlap of different labels. Second, unlike fluorescence probes SERS reporter groups do not self-quench, so that the intensity of the signal can be enhanced by increasing the number of SERS reporter groups.[50] Dou et al.[51] developed a new enzyme immunoassay based on SERS. In their system, antibody immobilized on a solid substrate reacts with antigen, which binds with another antibody labeled with peroxidase (POD). If this immunocomplex is subjected to the reaction with orthophenylenediamine and hydrogen peroxide, azoaniline is generated.[51] This azocompound is adsorbed on a Ag colloid, giving strong SERS signals. Porter et al.[54,55] proposed an immunoassay readout method based on SERS in a dual analyte sandwich assay. This method exploits SERS-derived signals from extrinsic three different reporter molecules that are coimmobilized with biospecific species on Au colloids.

We recently proposed a novel immunoassay based on SERS and immunogold labeling with Ag staining enhancement.[59] Immunoreactions between immunogold colloids modified by Raman-active probe molecules [e.g., 4-mercaptobenzoic acid (MBA)] and antigens, which were captured by antibody-assembled chips, were detected *via* SERS signals of Raman-active probe molecules. The immunoassay was performed by a sandwich structure. After Ag staining enhancement, the antigen is identified by a SERS spectrum of MBA. A working curve of the intensity of a SERS signal at 1585 cm^{-1} due to the ν_{8a} aromatic ring vibration of MBA versus the concentration of antigen was obtained and the nonoptimized detecting limit for the Hepatitis B virus surface antigen (Antigen) was found to be as low as 5 $\times 10^{-4}$ mg/mL.[59]

This review paper consists of four parts. The first part is concerned with the enzyme immunoassay based on the indirect SERS method proposed by Dou et al.[51] In this immunoassay, antibody immobilized on a solid substrate reacts with antigen, which binds with another antibody labeled with POD.[51] The second part reports a near-infrared (NIR) SERS technique that directly detects the immune reaction on the Au colloidal nanoparticles without any procedure for bound/free (B/F) separation.[53] The third part describes the new immunoassay using probe-labeling immunogold with Ag staining enhancement *via* SERS technique, which has been used for the quantitative detection of Antigen by means of a sort of
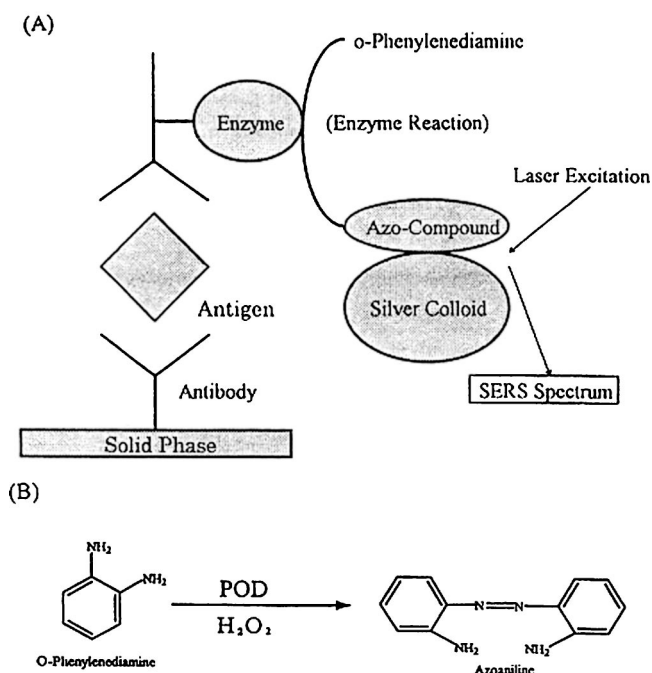
Fig. 1 (a) Enzyme immunoassay based upon indirect SERS method and (b) enzyme reaction investigated.

self-assembled sandwich structure immobilized on a silicon or quartz substrate.[59] The last part discusses the improvement of the immunogold nanolabeling and Ag staining enhancement method described in the third part.[95,96] In the improved method, the Au/Ag immunocoreshell nanoparticles instead of the immunogold nanoparticles are used as the labels in this sandwich immunoassay system and the procedure of Ag staining enhancement is avoided.

Part 1—Enzyme Immunoassay by Indirect Surface-Enhanced Raman Scattering Method

Dou et al.[51] proposed an enzyme immunoassay utilizing indirect SERS method. The detection limit of this system was found to be about 10^{-7} mg/mL, which was lower by one-order than that of the system employed by Cotton et al.[50] The proposed system is illustrated in Fig. 1.[51] In this system, antibody immobilized on a solid substrate reacts with antigen which binds with another antibody labeled with POD. When this immunocomplex is reacted with orthophenylenediamine and hydrogen peroxide, azoaniline is generated as a reaction product (Fig. 1). SERS signals from azoaniline absorbed on Ag colloid are measured to estimate the concentration of antigen [mouse-Immunoglobulin G (IgG)]. The SERS reporter group of this system is a simple and stable dye that show very strong Raman bands due to the N=N and C=C stretching modes. Moreover, the selectivity is extremely high because only the dye yields SERS signals. Of note in this system is that the concentration of antigen is determined indirectly via the SERS signals of the reaction product. Therefore, the sensitivity of the method is free from the Raman scattering intensity of the label directly attached to antibody. This method was named the indirect SERS method.[51]

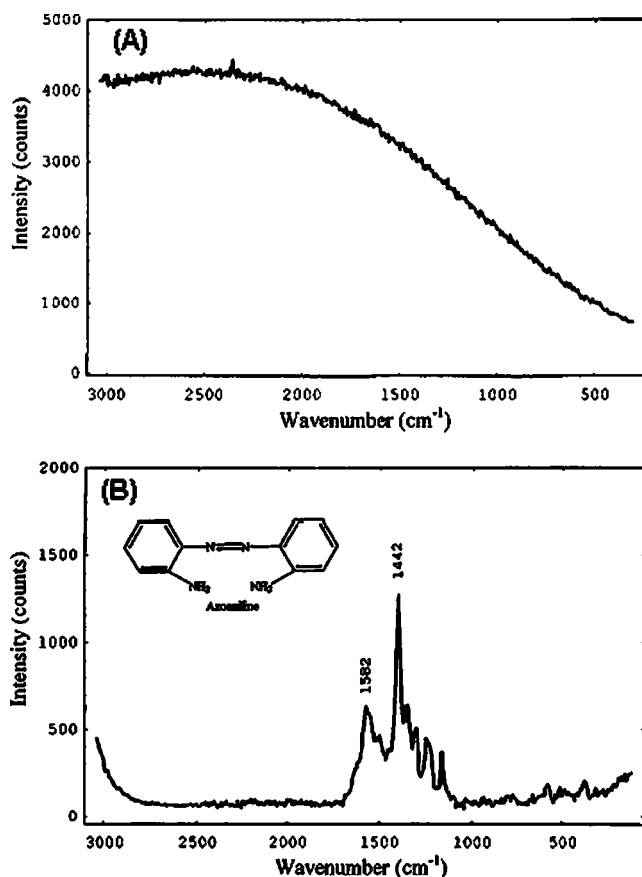Figure 2(a) shows a normal Raman spectrum of the reac-

Fig. 2 (a) A normal Raman spectrum of the reaction product (azoaniline) of the enzyme reaction shown in Fig. 1. (b) A SERS spectrum of the enzyme-substrate mixture after the reaction.

tion mixture of 10^{-6} mol/L orthophenylenediamine, 0.1% POD, and 0.136% hydrogen peroxide after the enzyme reaction.[51] Note that the spectrum shows strong fluorescent background. A SERS spectrum of the reaction mixture of the above three compounds is shown in Fig. 2(b).[51] Before we applied the SERS method to the enzyme reaction mixture, SERS spectra had been measured for 10^{-6} mol/L orthophenylenediamine, 0.1% POD, and 0.136% hydrogen peroxide, separately,[51] and we had confirmed that no peak was observed in the obtained spectra expect for a weak feature around 1650 cm^{-1} due to water. Therefore, there is little doubt that the SERS signals in the spectrum of Fig. 2(b) arise from the enzyme product generated by the oxidation-condensation reaction of orthophenylenediamine. Of particular importance is that only the enzyme reaction product yields strong SERS signals and that the enzyme or substrate itself does not show any detectable SERS peak. In other words, the concentration of the product can be monitored selectively without any interference. It is also noted that the strong fluorescent background is markedly reduced in the SERS spectrum [compare Figs. 2(a) and 2(b)]. Bands at 1582 and 1442 cm^{-1} are due to the C=C and N=N stretching modes, respectively.

SERS spectra of azoaniline produced by the enzyme reaction of orthophenylenediamine with peroxide and the immunocomplex labeled by POD are displayed in Fig. 3.[51] The concentration of the antigen was changed from 1.575
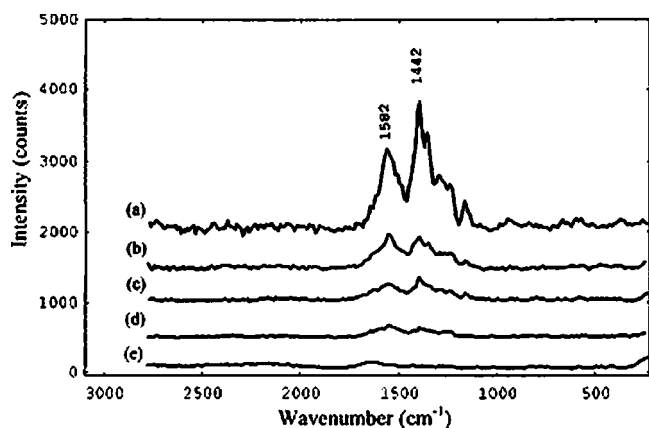
Fig. 3 SERS spectra of the reaction product of orthophenylenediamine with the immunocomplex labeled with POD. The concentration of antigen was 2.50 (a), 0.625 (b), 0.315 (c), and 0.1575 (d) ng/mL. The trace (e) is the spectrum of water.

Fig. 4 (a) Antibody adsorbed on Au colloid particle. (b) Immune complex on Au colloid particle.

$\times 10^{-7}$ mg/mL [Fig. 3(d)] to 2.5×10^{-6} mg/mL [Fig. 3(a)]. A good straight line was obtained between the intensity of the band at 1442 cm^{-1} versus the concentration of antigen. The correlation coefficient (R) between them was calculated to be 0.999 for the concentration range from 1.58×10^{-7} to 2.5×10^{-6} mg/mL.[51] The detection limit of this SERS enzyme immunoassay method was found to be about 10^{-7} mg/mL, which was lower by one order of magnitude than that found for a previously reported method employing SERS.[51] Even higher sensitivity might be expected if one could find more proper enzyme reaction system containing immunocomplexes because the sensitivity of this method is not controlled by Raman intensity of reporter molecules covalently bounded with antibody.

Part 2—Detection of Immune Reaction Without Bound/Free Antigen Separation by Near-Infrared Surface-Enhanced Raman Scattering

Almost all immunoassays currently being employed are so-called heterogeneous immunoassays that request a procedure for the separation of B/F antigens. However, the B/F separation is a rather cumbersome procedure and reagent consuming. We showed that NIR SERS spectroscopy holds considerable promise in detecting the immune reaction on the Au colloid particles without any procedure for the B/F separation.[53] The procedure for this method is illustrated in Figs. 4(a) and 4(b).[53] Antibody and immune complex are adsorbed on Au colloid particles. In the system free antigens cannot be adsorbed on the Au colloid surface, because the surface of the Au colloid particles is blocked by bovine serum albumin (BSA). A SERS spectrum of antimouse IgG at 2.2×10^{-8} mol/L adsorbed on the Au colloid particles shows a number of Raman bands due to amide groups and aromatic acid residues of antimouse IgG. A SERS spectrum of the same system at 1.9×10^{-10} mol/L does not give any SERS signal. However, Raman bands again appeared after the reaction of antimouse IgG at 1.9×10^{-10} mol/L with the antigen on the Au colloid particles.[53]

Figures 5(a) and 5(b) show NIR–SERS spectra of the Au colloid solution and antimouse IgG of 2.2×10^{-8} mol/L ad-
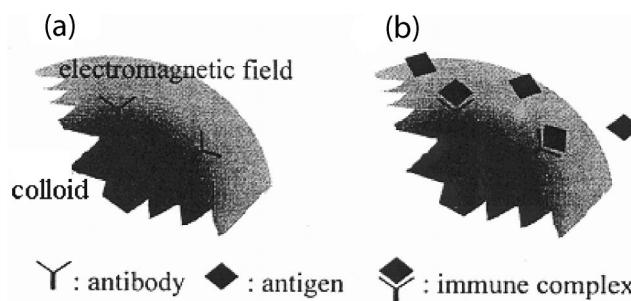
sorbed on the Au colloid particles, respectively.[53] The spectrum of antimouse IgG has an appearance fairly different from that of a typical protein Raman spectrum.[97] However, bands due to the amide groups (1645 and 1261 cm^{-1}) and those assignable to tryptophan (Trp) residues (1467, 1112, and 880 cm^{-1}) are clearly identified in the SERS spectrum of Fig. 5(b). Table 1 summarizes the frequencies and assignments of observed Raman bands. It is noted that the bands due to Trp are enhanced largely. According to previous SERS studies of proteins without a prosthetic group,[30,98–100] bands due to amide I and III are relatively weak in the SERS spectra of proteins, but those due to Trp and tyrosine residues (Tyr) appear strongly. It is also important to point out that the SERS spectra of proteins vary markedly with experimental conditions. For example, a SERS spectrum of BSA adsorbed on a Ag electrode with the potential corresponding to zero charge for Ag is different from that of BSA adsorbed on colloidal Ag at pH 8.0.[98,100] In this study, a 0.01 mol/L phosphate-crtrate buffer (pH$= 7.0$) containing a 0.005 mol/L NaCl solution has employed throughout the experiments, and all the SERS spectra were obtained under such experimental conditions.

The spectrum in Fig. 5(b) provides very interesting information about the adsorption of the protein on the Au
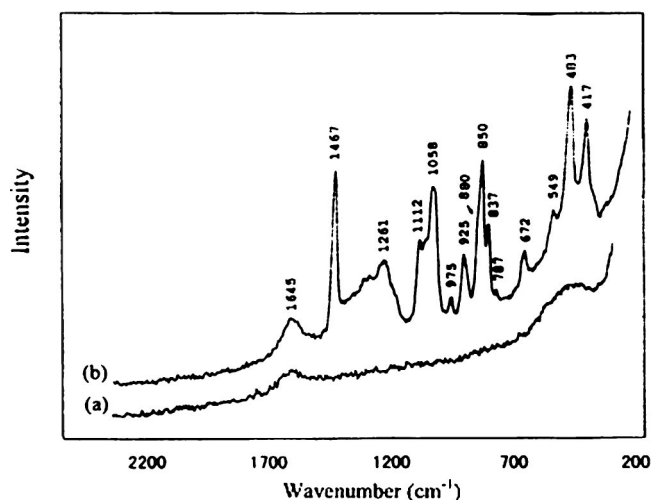

Fig. 5 (a) A NIR SERS spectrum of the Au colloid solution. (b) A NIR SERS spectrum of antimouse IgG of 2.2×10^{-8} mol/L adsorbed on Au colloid particles. Radiation of 1064 nm from an Nd:yttrium–aluminum–garnet laser was used as the excitation source, and the power at the sample point was typically 100 mW.

Table 1 Wave numbers and assignments of SERS bands observed for antimouse IgG on the Au colloid particles (see Ref. 53).

SERS/cm^{-1}	Assignments
1645	Amide I+water
1467	Trp
1261	Amide II
1112	Trp
1058	
925	Trp
880	Trp
850	Tyr
837	Tyr
672	Trp or C–S
549	
483	
417	Trp

colloids.[53] The amide I and III bands appear at 1645 and 1261 cm^{-1}, respectively, which are typical frequencies for α-helix structure of a protein.[97] However, IgG has β sheet-rich structure, and, in fact, their amide I and III bands are observed at 1673 and 1239 cm^{-1} in the normal Raman spectra.[101,102] Therefore, it seems that the bands due to the α-helix parts of the antimouse IgG are particularly enhanced in the SERS spectrum. This indicates that the α-helix parts are closer to the surface of Au colloid particles.[53]

Figure 6(a) shows a NIR SERS spectrum of antimouse IgG of 1.9×10^{-10} mol/L adsorbed on the Au colloid particles.[53]
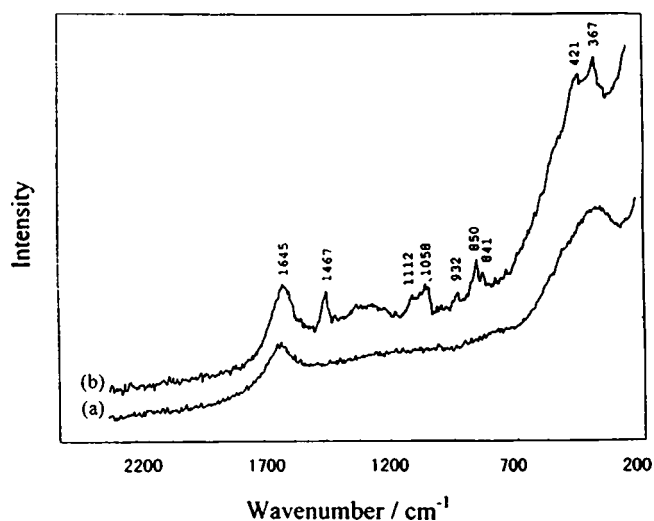

Fig. 6 (a) A NIR SERS spectrum of antimouse IgG of 1.9×10^{-10} mol/L adsorbed on Au colloid particles. (b) A NIR SERS spectrum of IgG–antimouse IgG complex on Au colloid particles.

The Raman bands observed in the SERS spectrum of Fig. 5(b) disappear completely probably because the concentration of antimouse IgG was diluted by 100 times. Figure 6(b) depicts a NIR SERS spectrum of IgG–antimouse IgG complex on the Au colloid particles.[53] Raman bands again emerge, although they are weak. Note that the frequencies of those bands are very close of those of the Raman bands in the spectrum shown in Fig. 5(b). It seems that all the observed bands arise from the antibody part of IgG–antimouse IgG complexes adsorbed on the Au colloid particles.[53] In the system shown in Fig. 4 the only antibody part can be adsorbed directly on the Au surface, giving the SERS signals. Bound and free antigens do not show significant Raman bands since free antigen molecules are blocked by BSA molecules and bound antigen molecules are adsorbed indirectly on the Au surface. The proposed method allows one to detect a trace amount of immune complex on Au colloid particles without any need for the B/F separation. It was also concluded from the earlier study that the configuration of antimouse IgG is modified significantly upon the reaction of antigen with antimouse IgG on the colloid particles, emerging intense SERS signals.[53]

Part 3—Immunoassay Using Probe-Labeling Immunogold Nanoparticles With Ag Staining Enhancement via Surface-Enhanced Raman Scattering

We recently proposed a novel immunoassay based on SERS and immunogold labeling with Ag staining enhancement.[59] This is also an indirect SERS method. Immunoreactions between immunogold colloids modified by a Raman-active probe molecule (e.g., MBA) and antigens, which were captured by antibody-assembled chips such as silicon or quartz, were detected *via* SERS signals of Raman-active probe molecules.[59] It was found that the nonoptimized detection limit for Antigen is as low as 5×10^{-4} mg/mL.[59]

Figure 7 illustrates the proposed system. The immunoassay is performed by a sandwich structure consisting of three layers. The first layer is composed of immobilized antibody molecules of mouse polyclonal antibody against Hepatitis B virus surface antigen (PAb) on a silicon or quartz substrate. The second layer is the complementary Antigen molecules captured by PAb on the substrate. The third layer consists of the probe-labeling immunogold nanoparticles, which have been modified by mouse monoclonal antibody against Hepatitis B virus surface antigen (MAb) and MBA as the Raman-active probe on the surface of Au colloids. After Ag staining enhancement, Antigen is identified by a SERS spectrum of MBA.

In this system, all the self-assembled steps were subjected to the measurements of AFM to monitor the formation of a sandwich structure onto a substrate.[103] Figure 8 shows AFM height images of each immobilized step on silicon microchips.[59] These AFM images suggest that the Antigen molecules execute the immuno-identification with the PAb molecules and are firmly captured by the (3-aminopropyl)trimethoxysilane (APTMS)-glutaraldehyde (GA)-PAb-Antigen substrate. The immunogold nanoparticles are also strongly bound to the surface through the immuno-identification. After Ag staining, a layer of Ag film covers the surface of the sandwich self-assembled multilayer.
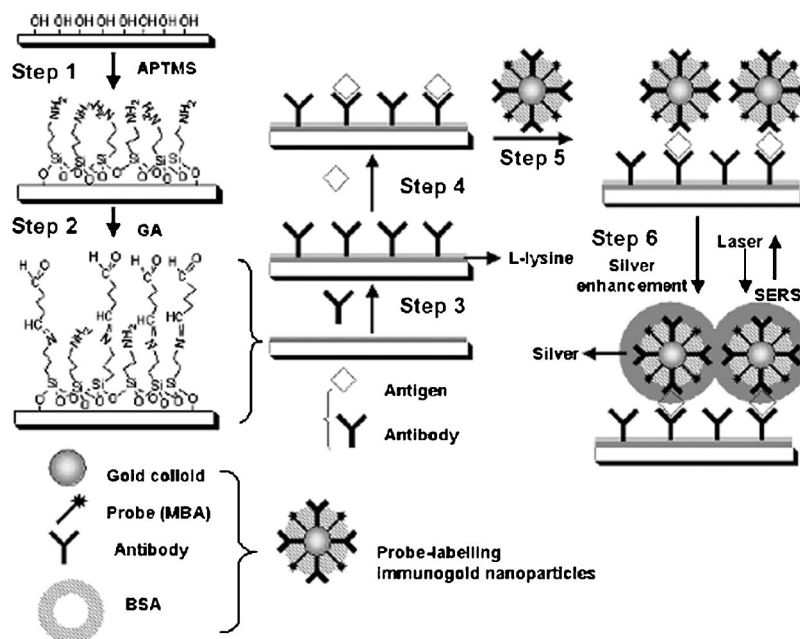
Fig. 7 The process of self-assembled sandwich structure immobilized on a silicon or quartz substrate using MBA-labeling immunogold nanoparticles with the Ag staining enhancement method.

The spectral features of MBA in SERS spectra can confirm the selective immunoassays. Figure 9 shows SERS spectra of MBA adsorbed on the immunogold nanoparticles after the Ag staining enhancement.[59] The Antigen solutions with different concentrations of 0, 0.5, 1, 2, 10, 20, 40, and 50 $\times 10^{-3}$ mg/mL were examined by the method depicted in Fig. 7, and their SERS spectra are shown in Figs. 9(a)–9(h), respectively. Strong SERS bands at 1585 and 1076 cm^{-1} are assigned to ν_{8a} and ν_{12} aromatic ring vibrations, respectively.[104] Figure 10 illustrates the relationship between the intensity of the peak at 1585 cm^{-1} and the concentration of Antigen. We developed a calibration model that predicts
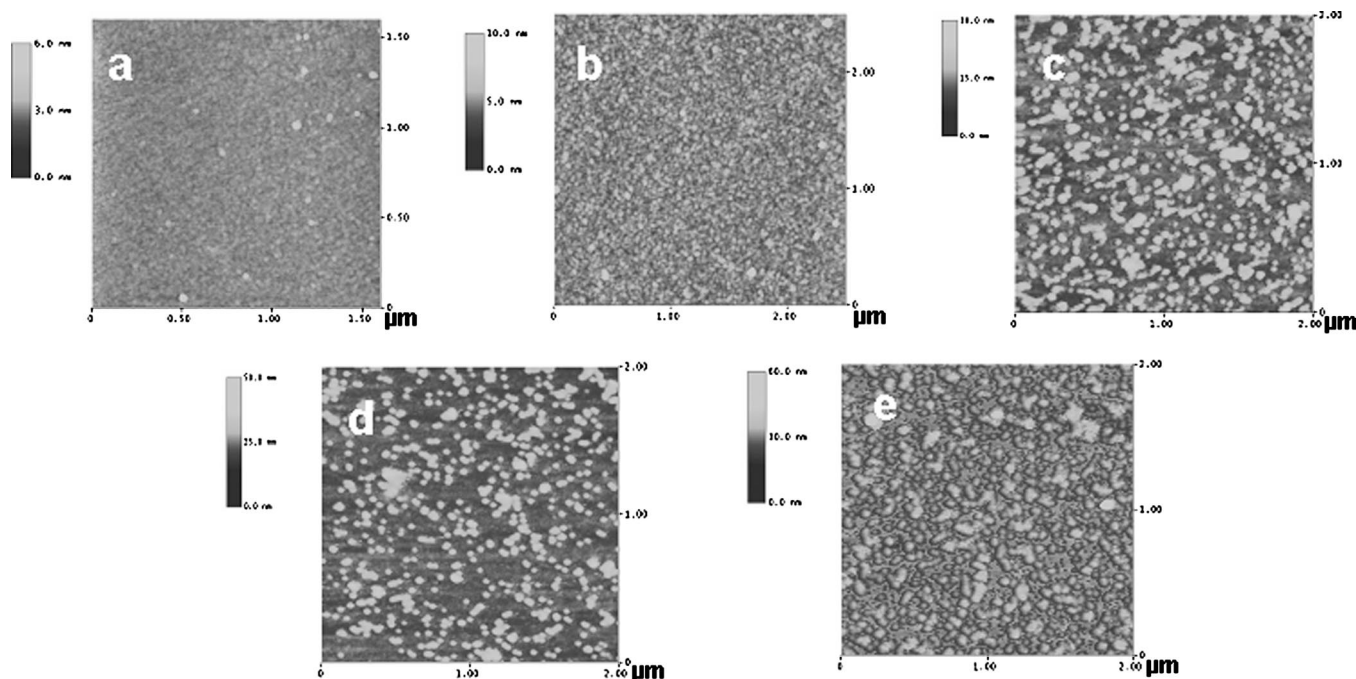

Fig. 8 AFM height images of one by one immobilized steps on silicon microchips. (a) an APTMS-GA surface; (b) an APTMS-GA-PAb surface; (c) an APTMS-GA-PAb-Antigen surface, where the concentration of the Antigen was 100 μg/mL; (d) an APTMS-GA-PAb-Antigen-Immunogold surface, where the concentration of the Antigen was 0.1 mg/mL; (e), the same as (d), but after Ag staining enhancement; (a) 1.5 μm$\times$1.5 μm; (b)–(e) 2 μm$\times$2 μm.
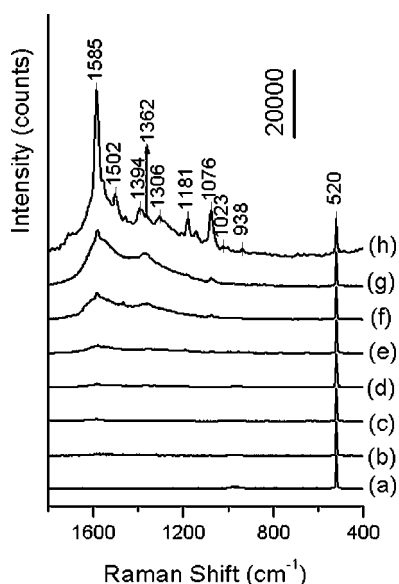
Fig. 9 SERS immunoassay using MBA-labeling nanoparticles with the Ag staining enhancement method. Antigen with concentrations of 0, 0.5, 1, 2, 10, 20, 40, and 50 $\times 10^{-3}$ mg/mL was detected by this method, and their SERS spectra from 1800 to 400 cm^{-1} are shown in (a), (b), (c), (d), (e), (f), (g), and (h), respectively. All the spectra were dealt with the normalized operations assuming the intensity of the peak at 520 cm^{-1} due to silicon as the intensity of 10 000.

Fig. 11 SERS spectra of MBA in immunoassay using the MBA-labeling immunogold nanoparticles. (a) before and (b) after the Ag staining enhancement. The detection limit of Antigen was as low as 0.5 $\times 10^{-3}$ mg/mL. The spectra were dealt with the normalized operations assuming the intensity of the peak at 520 cm^{-1} due to silicon as the intensity of 10 000.

the concentration of Antigen in the range of 1–40 $\times 10^{-3}$ mg/mL. The inset of Fig. 10 depicts the model; the R and standard deviation are 0.98 ($n=5$) and 214, respectively, and the unoptimized detecting limit of Antigen is as low as 5×10^{-4} mg/mL.

One must notice in Fig. 9(h) that the SERS signals of MBA show unusually strong when the Antigen concentration is 5×10^{-4} mg/mL. This is probably because at a high concentration, there are more immunogold nanoparticles on the slide surface due to the immunoreaction. Therefore, many immunogold nanoparticles lead to a great deal of Ag aggregates
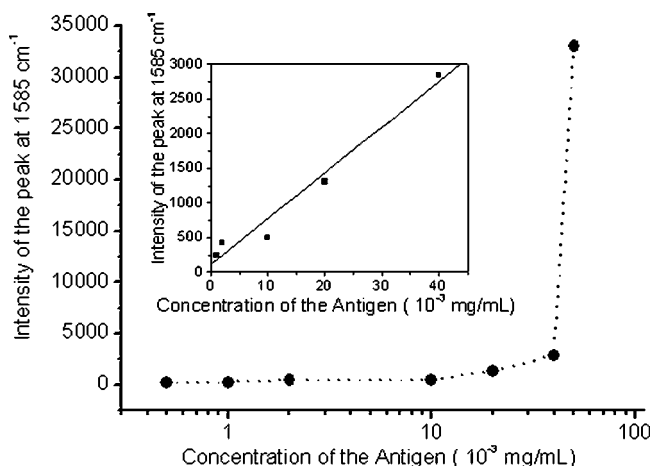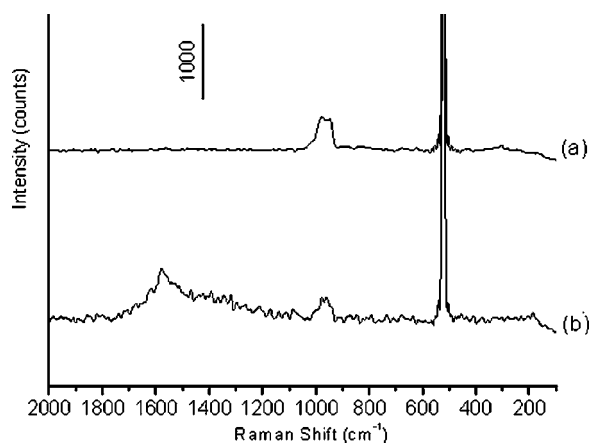
onto the surface after the Ag staining. The large aggregates can remarkably enhance the SERS signals much more strongly than a single nanoparticle according to the electronic field theory of SERS.[105] Therefore, the SERS signal increase remarkably in Figs. 9(h) and 10.

Figure 11 shows SERS spectra of MBA on the APTMS-GA-PAb-Antigen-immunogold substrate where the concentration of Antigen is as low as 5×10^{-4} mg/mL before (a) and after (b) the Ag staining enhancement.[59] After the Ag staining enhancement, the Raman signals are increased by 10–100 times, thereby improving the detection sensitivity of this immunoassay method.

This method has combined the advantages of the SERS technique with those of the nanolabeling method.[59] The advantages of the immunogold nanoparticles, such as their easily controllable-size distribution, long-term stability, and friendly biocompatibility confirm the reproducibility of the immunoassay.

Part 4—Immunoassay Using Probe-Labeling Au/Ag Immunocoreshell Nanoparticles via Surface-Enhanced Raman Scattering

In the immunoassay described in Part 3, the Ag staining method plays an important role; it can remarkably enhance Raman signals by several decuples, improving the detecting sensitivity of the immunoassay. However, the reduced Ag film covers the surface of the APTMS-GA-PAb-Antigen-immunogold substrate, and thus the bioactivity of the antibodies and antigens may be destroyed significantly. Therefore, we developed a new label that possesses both SERS enhancing ability and good biocompatibility. We used the Au/Ag immunocoreshell nanoparticles instead of the immunogold nanoparticles as the labels in the above sandwich immunoassay system.[95,96]

The experimental procedure in Part 4 is mostly the same as that mentioned in Part 3. The immunoassay was also performed by a sandwich structure consisting of three layers. It should be pointed out that the third layer is composed of the
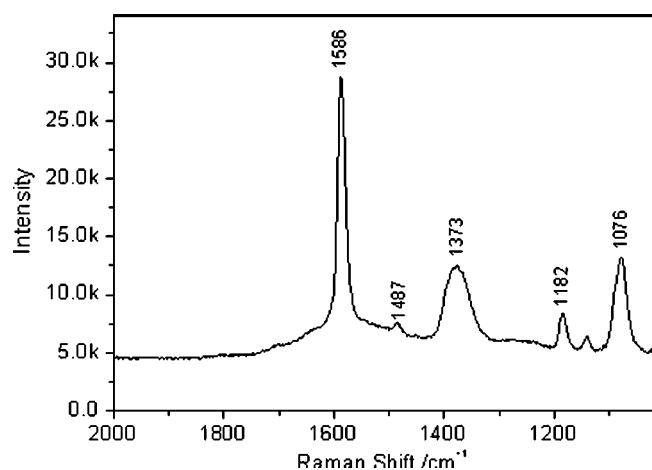

Fig. 10 The relationship between the intensity of the SERS signal at 1585 cm^{-1} and the concentration of Antigen. Inset: a calibration model that predicts the concentration of Antigen in the range from 1 to 40 $\times 10^{-3}$ mg/mL.

Fig. 12 A SERS spectrum of MBA added into the Au/Ag coreshell colloid.

MBA-labeling Au/Ag immunocoreshell nanoparticles. The MBA-labeling Au/Ag immunocoreshell nanoparticles were prepared by the following four steps. First, the Au/Ag coreshell nanoparticles were prepared according the literature.[106] In a typical process, 5 mL of 10^{-3} mol/L Au colloids was diluted to 95 mL, and then 1.0 mL of a 1% trisodium citrate solution was added to the earlier solution. After heating the solution to boil temperature, 5.0 mL of 0.01 mol/L $AgNO_3$ was added under continuous stirring to produce the desired final bimetallic colloids. To prevent the formation of separate Ag particles, 0.5 mL $AgNO_3$ solution was added each 5 min. The coreshell nanoparticles used have a 13-nm-diameter Au core that is coated by an 8-nm-thick Ag shell. Second, 4 μL of MBA in methanol (1×10^{-3} mol/L) was added as the Raman-active probe to 1.0 mL of Au/Ag core-shell colloids. After 12 h standing under stirring, the MBA modified Au/Ag core-shell colloids were purified by centrifugation and resuspended with 1.0 mL borate buffer (2 mM, pH=9). As the third step, 5 μL of MAb (2.0 mg/mL) PBS buffer solution (a PBS buffer solution; KH_2PO_4/K_2HPO_4, pH=7.4) was added to 1.0 mL MBA-labeling Au/Ag coreshell colloid. The amount of MAb we added into the MBA-labeling Au/Ag coreshell colloid was 50% more than the minimum amount for coating the unmodified portion of the colloid surface. Finally, to assure that no space around the surface of coreshell colloids was left, 10 μL of BSA (2% m/m) solution was added to the mentioned MBA-labeling Au/Ag coreshell colloid, to occupy the un-coated place.

Figure 12 shows a SERS spectrum of MBA measured when MBA was added into the Au/Ag coreshell colloid. From Fig. 12, one can see that the Au/Ag coreshell nanoparticles have strong SERS activity.[106] We again used AFM to confirm the self-assembled step (see Fig. 13). It can be seen from the section analysis of AFM images in Fig. 13 that the biomolecules and the Au/Ag immunocoreshell nanoparticles form many compacted islands on the silica substrate. The height and diameter of the islands change obviously at each immobilized step. It is clear that the Au/Ag immunocoreshell nanoparticles have been successfully immobilized onto the surface of APTMS-GA-PAb-Antigen by the immunoreaction.
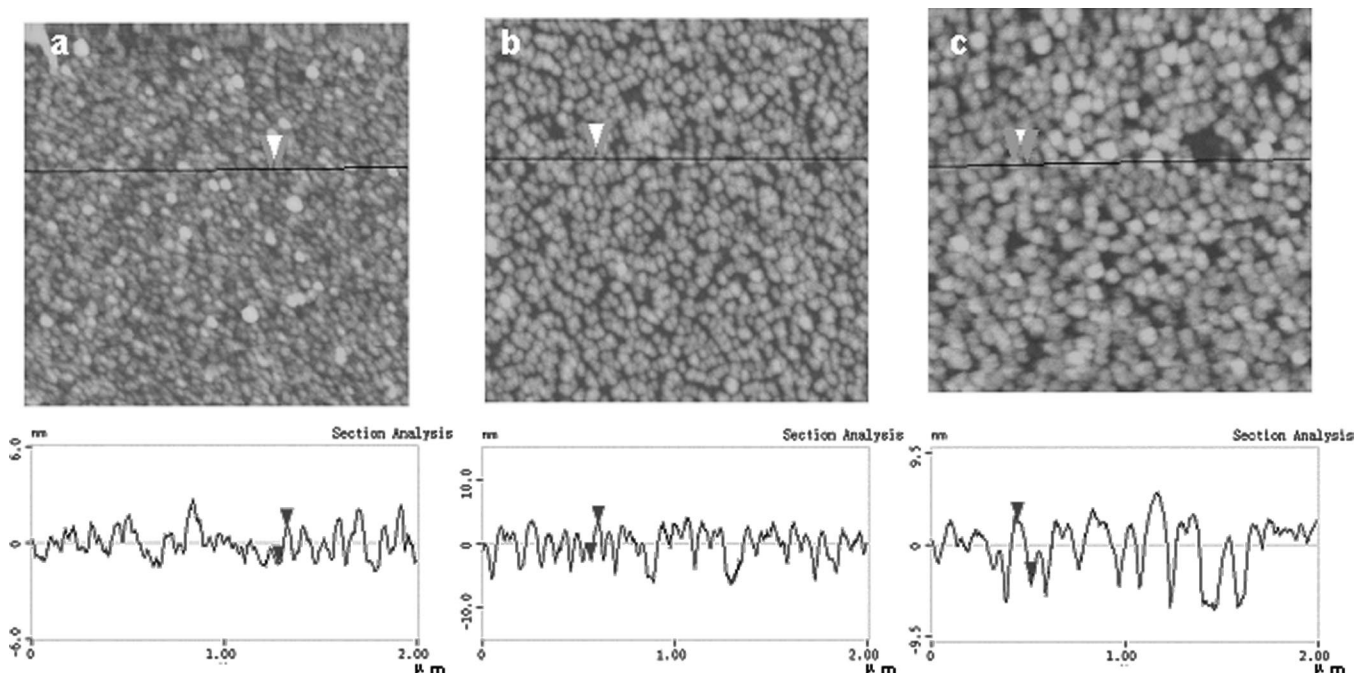

Fig. 13 AFM height images of one by one immobilized steps on silicon microchips. (a) A surface after the PAb immobilized on the APTMS-GA substrate, with the horizontal distance between two triangle symbol is 43.0 nm and the vertical distance is 2.3 nm; (b) a surface after the Antigen captured by PAb of the substrate, with the horizontal distance is 39.0 nm and the vertical distance is 5.7 nm; (c) a sandwich structure composed of the PAb, Antigen, and the Au/Ag immuno-coreshell nanoparticles with MBA-labeling, with the horizonal distance is 70.3 nm and the vertical distance is 6.1 nm. (a)–(c) 2 μm$\times$2 μm.
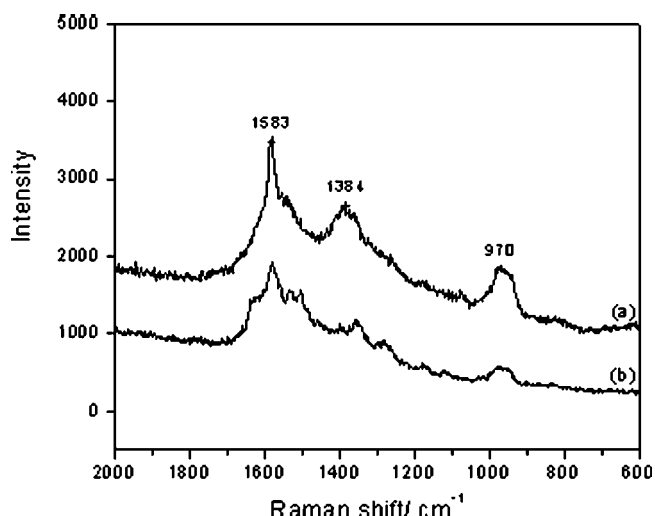
Fig. 14 SERS immunoassay with two kinds of the labeled methods. (a) using MBA-labeling Au/Ag immunocoreshell nanoparticles, (b) using the MBA-labeling immunogold nanoparticles with Ag staining enhancement.

Figure 14(a) depicts SERS signals of MBA in this sandwich immunoassay system where the concentration of Antigen is 0.02 mg/mL. Most of strong SERS bands are assigned to MBA. Figure 14(b) shows a SERS spectrum of MBA measured by using the method mentioned in Part 3 with the same concentration of Antigen (0.02 mg/mL). Comparison of both spectra in Figs. 14(a) and 14(b) reveals that the MBA-labeling Au/Ag immunocoreshell nanoparticles used as labels are as useful as the Ag staining method in terms of the SERS enhancement. Note that the procedure method is simpler than the method described in Part 3.

The major difference between these two methods is that the Au/Ag coreshell nanoparticles are used to prepare the immunolabels instead of the Au nanoparticles. The SERS signals of MBA indicate that this Au/Ag coreshell nanoparticles have strong Raman band enhancing ability. Another important difference is that the Ag staining enhancement is avoided in the experimental procedure in Part 4. The advantages of the procedure without the Ag staining enhancement step are the simplification of the experiment procedure as well as the prolongation of bioactivity of the biomolecules after the SERS detection.

Conclusion

The application of SERS to immunoassay is one of the most promising topics among the SERS applications and has attracted a number of researchers. In this review paper, we present three immunoassay methods and one improvement via SERS. Table 2 compares the three SERS immunoassay methods investigated. Compared with the ELISA method having the detection limit of ng/mL to pg/mL,[76] the methods by Dou et al.[51,53] described in Parts 1 and 2 do not show any superiority on the detection limit. However, both methods have provided new immunoassay methods by SERS. Their advantages are mainly based on the characteristics of SERS. For example, the detection of the Part 1 method does rely on the concentration of the azodye, which is not covalently bound with the antibody. In other words, the concentration of antigen is determined indirectly via the SERS signals of the reaction product, the azodye. Therefore, the sensitivity of the method is free from the Raman scattering intensity of the label directly attached to antibody. The Part 2 method can provide the evidence for a slight modification of the configuration of antimouse IgG on the formation of an immune complex. This NIR SERS method holds considerable promise in detecting the immune reaction without any procedure for the B/F separation. These are the useful complements for the ELISA method. However, none of the SERS immunoassay methods proposed has been realized yet. The immunoassay methods using SERS reported in this review have been carried out only in laboratories. Further development of the studies on SERS mechanism, Raman instrumentation, nanotechnology, and

Table 2 Comparison of the three SERS immunoassay methods.

Methods	Detection limit	Characteristic features	Limitations	Ref.
SERS (indirect method)	$\sim 10^{-7}$ mg/mL	Multiple label-based detections	The narrow measurement range	51
NIR SERS (direct method)	$\sim 10^{-4}$ mg/mL*	Providing more structural information about the antibodies. No need for B/F separation. Direct detection.	Higher detection limit	53
SERS (indirect method)	5×10^{-4} mg/mL	Utilization of the metallic nano labels both in remarkable Raman-enhanced ability and in friendly biocompatibility	Higher detection limit	58, 59, 95, 96

* An approximate datum according to the amount of $(1.9 \times 10^{-4}$ mol/L) antimouse IgG.

novel ideas should make SERS real practical techniques not only in immunoassay but also various bioassay, clinical diagnosis, and environmental monitoring.

References

1. M. Jackson and H. H. Mantsch, "Pathology by infrared and Raman spectroscopy," in *Hand Book of Vibrational Spectroscopy Vol. 5: Applications in Life, Pharmaceutical and Natural Science*, J. M. Chalmers and P. R. Griffiths, Eds., pp. 3227–3245, Wiley, Chichester (2002).
2. *Handbook of Raman Spectroscopy: From the Research Laboratory to the Process Line*, I. R. Lewis and H. G. M. Edwards, Eds., Marcel Dekker, New York (2001).
3. G. J. Puppels and J. Greve, "Whole cell studies and tissue characterization by Raman spectroscopy," in *Biomedical Applications of Spectroscopy*, R. J. H. Clark and R. E. Hester, Eds., Chap. 1, pp. 1–47, Wiley, Chichester (1996).
4. L. A. Lyon, C. D. Keating, A. P. Fox, B. E. Baker, L. He, S. R. Nicewarner, S. P. Mulvaney, and M. J. Natan, "Raman spectroscopy," *Anal. Chem.* **70**, 341–362 (1998).
5. K. Kneipp, H. Kneipp, I. Itzkan, R. R. Dasari, and M. S. Feld, "Ultrasensitive chemical analysis by Raman spectroscopy," *Chem. Rev. (Washington, D.C.)* **99**, 2957–2975 (1999).
6. W. E. Smith and C. Rodger, "Surface-enhanced Raman spectroscopy," in *Hand Book of Vibrational Spectroscopy Vol. 1: Theory and Instrumentation*, J. M. Chalmers and P. R. Griffiths, Eds., pp. 775–784, Wiley, Chichester (2002).
7. *Surface-Enhanced Raman Scattering*, R. K. Chang and T. E. Furtak, Eds., Plenum, New York (1982).
8. M. Moskovits, "Surface-enhanced spectroscopy," *Rev. Mod. Phys.* **57**, 783–826 (1985).
9. A. Campion and P. Kambhampati, "Surface-enhanced Raman scattering," *Chem. Soc. Rev.* **2**, 241–249 (1998).
10. T. Vo-Dinh, "Surface-enhanced Raman spectroscopy using metallic nanostructures," *Trends Analyt. Chem.* **17**, 557–582 (1998).
11. S. Nie and S. R. Emory, "Probing single molecules and single nanoparticles by surface-enhanced Raman scattering," *Science* **275**, 1102–1106 (1997).
12. K. Kneipp, Y. Wang, H. Kneipp, L. T. Perelman, L. Ltzkan, R. R. Dasari, and M. S. Feld, "Single molecule detection using surface-enhanced Raman scattering (SERS)," *Phys. Rev. Lett.* **78**, 1667–1670 (1997).
13. *Biological Applications of Raman Spectroscopy*, T. G. Spiro, Ed., Wiley, New York (1988).
14. E. Koglin and J. M. Sequaris, "Surface enhanced Raman scattering of biomolecules," *Top. Curr. Chem.* **134**, 1–57 (1986).
15. R. F. Paisley and M. D. Morris, "Surface enhanced Raman spectroscopy of small biological molecules," *Prog. Anal. Spectrosc.* **11**, 111–140 (1988).
16. H. Fabian and P. Anzenbacher, "New developments in Raman spectroscopy of biological systems," *Vib. Spectrosc.* **4**, 125–148 (1993).
17. E. E. Lawson, B. W. Barry, A. C. Williams, and H. G. M. Edwards, "Biomedical applications of Raman spectroscopy," *J. Raman Spectrosc.* **28**, 111–117 (1998).
18. E. A. Carter and H. G. Edwards, "Biological applications of Raman spectroscopy," in *Infrared and Raman Spectroscopy of Biological Materials*, H.-U. Gremlich and B. Yan, Eds., pp. 421–475, Marcel Dekker, New York (2002).
19. X. M. Dou and Y. Ozaki, "Surface-enhanced Raman scattering of biological molecules on metal colloids: Basic studies and applications to quantitative assay," *Rev. Anal. Chem.* **18**, 285–321 (1999).
20. K. Kneipp, H. Kneipp, I. Itzkan, R. R. Dasari, and M. S. Feld, "Surface-enhanced Raman scattering and biophysics," *J. Phys.: Condens. Matter* **14**, R597–R624 (2002).
21. V. L. Schlegel and T. M. Cotton, "Silver-island films as substrates for enhanced Raman scattering: effect of deposition rate on intensity," *Anal. Chem.* **63**, 241–247 (1991).
22. S. R. Emory and S. M. Nie, "Screening and enrichment of metal nanoparticles with novel optical properties," *J. Phys. Chem. B* **102**, 493–497 (1998).
23. S. J. Suh and J. A. Moskovits, "Surface-enhanced resonance Raman scattering from cytochrome *c* and myoglobin adsorbed on a silver electrode," *J. Am. Chem. Soc.* **102**, 7960–7962 (1980).
24. T. M. Cotton, S. G. Schultz, and R. P. Van Duyne, "Surface-enhanced resonance Raman scattering from water-soluble porphyrins adsorbed on a silver electrode," *J. Am. Chem. Soc.* **104**, 6528–6532 (1982).
25. I. R. Nabiev, V. A. Savchenko, and E. S. Efremov, "Surface-enhanced Raman spectra of aromatic amino acids and proteins adsorbed by silver hydrosols," *J. Raman Spectrosc.* **14**, 375–379 (1983).
26. T. H. Joo, M. S. Kim, and K. Kim, "Surface-enhanced Raman scattering of benzenethiol in silver sol," *J. Raman Spectrosc.* **18**, 57–60 (1987).
27. D. Curley and O. Siiman, "Conformation and orientation of the haptens, 2,4-dinitrophenyl amino acids, on colloidal silver from surface-enhanced Raman scattering," *Langmuir* **4**, 1021–1032 (1988).
28. R. E. Holt and T. M. Cotton, "Surface-enhanced resonance Raman and electrochemical investigation of glucose oxidase catalysis at a silver electrode," *J. Am. Chem. Soc.* **111**, 2815–2821 (1989).
29. R. Picorel, R. E. Holt, T. M. Cotton, and M. Seibert, "Surface-enhanced resonance Raman scattering spectroscopy of bacterial photosynthetic membranes. The carotenoid of Rhodospirillum rubrum," *J. Biol. Chem.* **263**, 4374–4380 (1988).
30. G. D. Chumanov, R. G. Efremov, and I. R. Nabiev, "Surface-enhanced Raman-spectroscopy of biomolecules. 1. Water-soluble proteins, dipeptides and amino-acids," *J. Raman Spectrosc.* **21**, 43–48 (1990).
31. K. Sokolov, P. Khodorchenko, A. Petukhov, I. Nabiev, G. Chumanov, and T. M. Cotton, "Contributions of short-range and classical electromagnetic mechanisms to surface-enhanced Raman scattering from several types of biomolecules adsorbed on cold-deposited island films," *Appl. Spectrosc.* **47**, 515–522 (1993).
32. D. Graham, W. E. Smith, A. M. T. Linacre, C. H. Munro, N. D. Watson, and P. C. White, "Selective detection of deoxyribonucleic acid at ultralow concentrations by SERRS," *Anal. Chem.* **69**, 4703–4707 (1997).
33. X. Dou, Y. M. Jung, H. Yamamoto, S. Doi, and Y. Ozaki, "Near-infrared excited surface-enhanced Raman scattering of biological molecules on gold colloid I: Effects of *p*H of the solutions of amino acids and of their polymerization," *Appl. Spectrosc.* **53**, 133–138 (1999).
34. X. Dou, Y. M. Jung, Z. Cao, and Y. Ozaki, "Surface-enhanced Raman scattering of biological molecules on metal colloid II: Effects of aggregation of gold colloid and comparison of effects of *p*H of Glycine solutions between gold and silver colloids," *Appl. Spectrosc.* **53**, 1440–1447 (1999).
35. X. Y. Xiao, S. G. Sun, J. L. Yao, Q. H. Wu, and Z. Q. Tian, "Surface-enhanced Raman spectroscopic studies of dissociative adsorption of amino acids on platinum and gold electrodes in alkaline solutions," *Langmuir* **18**, 6274–6279 (2002).
36. E. J. Bjerneld, Z. Foldes-Papp, M. Kall, and R. Rigler, "Single-molecule surface-enhanced Raman and fluorescence correlation spectroscopy of horseradish peroxidase," *J. Phys. Chem. B* **106**, 1213–1218 (2002).
37. K. Niki and V. Brabec, "Raman scattering from nucleic acids adsorbed at a silver electrode," *Biophys. Chem.* **23**, 63–70 (1985).
38. K. Kneipp and J. Flemming, "Surface enhanced Raman scattering (SERS) of nucleic acids adsorbed on colloidal silver particles," *J. Mol. Struct.* **145**, 173–179 (1986).
39. K. Kneipp, W. Pohle, and H. Fabian, "Surface enhanced Raman spectroscopy on nucleic acids and related compounds adsorbed on colloidal silver particles," *J. Mol. Struct.* **244**, 183–192 (1991).
40. T. Vo-Dinh, K. Houck, and D. L. Stokes, "Surface-enhanced Raman gene probes," *Anal. Chem.* **66**, 3379–3383 (1994).
41. N. R. Isola, D. L. Stokes, and T. Vo-Dinh, "Surface-enhanced Raman gene probe for HIV detection," *Anal. Chem.* **70**, 1352–1356 (1998).

42. X. Dou, T. Takama, Y. Yamaguchi, K. Hirai, H. Yamamoto, S. Doi, and Y. Ozaki, "Quantitative analysis of double-stranded DNA amplified by a polymerase chain reaction employing surface-enhanced Raman spectroscopy," *Appl. Opt.* **37**, 759–763 (1998).

43. V. Deckert, D. Zeisel, R. Zenobi, and T. Vodinh, "Near-field surface-enhanced Raman imaging of dye-labeled DNA with 100-nm resolution," *Anal. Chem.* **70**, 2646–2650 (1998).

44. Y. D. Zhao, D. W. Pang, S. Hu, Z. L. Wang, J. K. Cheng, Y. P. Qi, H. P. Dai, B. W. Mao, Z. Q. Tian, J. Luo, and Z. H. Lin, "DNA-modified electrodes—Part 3—Spectroscopic characterization of DNA-modified gold electrodes," *Anal. Chim. Acta* **388**, 93–101 (1999).

45. D. Graham, B. J. Mallinder, and W. E. Smith, "Surface-enhanced resonance Raman-scattering as a novel method of DNA discrimination," *Angew. Chem., Int. Ed.* **39**, 1061–1065 (2000).

46. Y. W. C. Cao, R. Jin, and C. A. Mirkin, "Nanoparticles with Raman spectroscopic fingerprints for DNA and RNA detection," *Science* **297**, 1536–1540 (2002).

47. S. Sanchez-Cortes, R. M. Berenguel, A. Madejon, and M. Perez-Mendez, "Adsorption of polyethyleneimine on silver nanoparticles and its interaction with a plasmid DNA: A surface-enhanced Raman scattering study," *Biomacromolecules* **3**, 655–660 (2002).

48. M. Culha, D. Stokes, L. R. Allain, and T. Vo-Dinh, "Surface-enhanced Raman scattering substrate based on a self-assembled monolayer for use in gene diagnostics," *Anal. Chem.* **75**, 6196–6201 (2003).

49. B. N. Rospendowski, J. M. Campbell, J. Reglinski, and W. E. Smith, "Direct spectroscopic determination of functional sulfhydryl-groups on intact cell-surfaces by surface-enhanced resonance Raman-scattering," *Eur. Biophys. J.* **21**, 257–261 (1992).

50. T. E. Rohr, T. Cotton, N. Fan, and P. J. Tarcha, "Immunoassay employing surface-enhanced Raman spectroscopy," *Anal. Biochem.* **182**, 388–398 (1989).

51. X. Dou, T. Takama, Y. Yamaguchi, H. Yamamoto, and Y. Ozaki, "Enzyme immunoassay utilizing surface-enhanced Raman scattering of the enzyme reaction product," *Anal. Chem.* **69**, 1492–1495 (1997).

52. S. R. Hawi, S. Rochanakij, F. Adar, W. B. Campbell, and K. Nithipatikom, "Detection of membrane bound enzymes in cells using immunoassay and Raman microspectroscopy" *Anal. Biochem.* **259**, 212–217 (1998).

53. X. Dou, Y. Yamaguchi, H. Yamamoto, S. Doi, and Y. Ozaki, "NIR SERS detection of immune reaction on gold colloid particles without bound/free antigen separation," *J. Raman Spectrosc.* **29**, 739–742 (1998).

54. J. Ni, R. J. Lipert, G. Dawson, and M. D. Porter, "Immunoassay readout method using extrinsic Raman labels adsorbed on immunogold colloids," *Anal. Chem.* **71**, 4903–4908 (1999).

55. D. S. Grubisha, R. J. Lipert, H.-Y. Park, J. Driskell, and M. D. Porter, "Femtomolar detection of prostate-specific antigen: an immunoassay based on surface-enhanced Raman scattering and immunogold labels," *Anal. Chem.* **75**, 5936–5943 (2003).

56. N. H. Kim, S. J. Lee, and K. Kim, "Isocyanide and biotin-derivatized Ag nanoparticles: An efficient molecular sensing mediator *via* surface-enhanced Raman spectroscopy," *Chem. Commun. (Cambridge)* **6**, 724–725 (2003).

57. Y. C. C. Cao, R. Jin, J. M. Nam, C. S. Thaxton, and C. A. Mirkin, "Raman dye-labeled nanoparticle probes for proteins," *J. Am. Chem. Soc.* **125**, 14676–14677 (2003).

58. S. P. Xu, L. Y. Wang, W. Q. Xu, B. Zhao, H. Yuan, L. Ma, Y. B. Bai, and Y. G. Fan, "Immunological identificaion with SERS-labeled immunogold nanoparticles by silver staining," *Chem. J. Chinese Universities* **24**, 900–902 (2003).

59. S. P. Xu, X. H. Ji, W. Q. Xu, X. L. Li, L. Y. Wang, Y. B. Bai, B. Zhao, and Y. Ozaki, "Immunoassay using probe-labelling immunogold nanoparticles with silver staining enhancement *via* surface-enhanced Raman scattering," *Analyst (Cambridge, U.K.)* **129**, 63–68 (2004).

60. H. Morjani, J. F. Riou, I. Nebiev, F. Lavelle, and M. Manfait, "Molecular and cellular interactions between intoplicine, DNA, and topoisomerase II studied by surface-enhanced Raman scattering spectroscopy," *Cancer Res.* **53**, 4784–4790 (1993).

61. I. R. Nabiev, H. Morjani, and M. Manfait, "Selective analysis of antitumor drug interaction with living cancer cells as probed by surface-enhanced Raman spectroscopy," *Eur. Biophys. J.* **19**, 311 (1991).

62. A. Bonifacio, D. Millo, C. Gooijer, R. Boegschoten, and G. Zwan, "Linearly moving low-volume spectroelectrochemical cell for microliter-scale surface-enhanced resonance Raman spectroscopy of

63. heme proteins," *Anal. Chem.* **76**, 1529–1531 (2004).

63. G. Sakai, K. Ogata, T. Uda, N. Miura, and N. Yamazoe, "Evaluation of binding of human serum albumin (HSA) to monoclonal and polyclonal antibody by means of piezoelectric immunosensing technique," *Sens. Actuators B* **49**, 5–12 (1998).

64. M. D. Darren, C. C. David, Y. Hong-Xing, and R. L. Christopher, "Covalent coupling of immunoglobulin G to self-assembled monolayers as a method for immobilizing the interfactial recognition layer of a surface plasmon resonance immunosensor," *Biosens. Bioelectron.* **13**, 1213–1225 (1998).

65. S. Toyama, A. Shoji, Y. Yoshida, S. Yamauchi, and Y. Ikariyama, "Design and characterization of polymer matrix anchored to gold thin layer for the effective surface design of SPR-based immunosensor for the effective binding of antigen or antibody in the evanescent field using mixed polymer matrix," *Sens. Actuators B* **52**, 65–71 (1998).

66. B. K. Oh, Y. K. Kim, W. Lee, Y. M. Bae, W. H. Lee, and J. W. Choi, "Immunosensor for detection of Legionella pneumophila using surface plasmon resonance," *Biosens. Bioelectron.* **18**, 605–611 (2003).

67. G. U. Lee, D. A. Kidwell, and R. J. Colton, "Sensing discrete streptavidin-biotin interactions with atomic force microscopy," *Langmuir* **10**, 354–357 (1994).

68. V. T. Moy, E. L. Florin, and H. E. Gaub, "Intermolecular forces and energies between ligands and receptors," *Science* **266**, 257–259 (1994).

69. U. Dammer, M. Hegner, D. Anselmetti, P. Wagner, M. Dreier, W. Huber, and H.-J. Guntherodt, "Specific antigen/antibody interactions measured by force microscopy," *Biophys. J.* **70**, 2437–2441 (1996).

70. V. W. Jones, J. R. Kenseth, and M. D. Porter, "Microminiaturized immunoassays using atomic force microscopy and compositionally patterned antigen arrays," *Anal. Chem.* **70**, 1233–1241 (1998).

71. M. C. Coen, R. Lehmann, P. Gröning, M. Bielmann, C. Galli, and L. Schlapbach, "Adsorption and bioactivity of protein A on silicon surfaces studied by AFM and XPS," *J. Colloid Interface Sci.* **233**, 180–189 (2001).

72. L. Li, S. Chen, S. Oh, and S. Jiang, "*In situ* single-molecule detection of antibody-antigen binding by tapping-mode atomic force microscopy," *Anal. Chem.* **74**, 6017–6022 (2002).

73. C. R. Suri, P. K. Jain, and G. C. Mishra, "Development of PZ crystal based microgravimetri immunoassay for determination of insulin concentration," *J. Biotechnol.* **39**, 27–34 (1995).

74. K. Nakanishi, H. Muguruma, and I. Karube, "A novel method of immobilizing antibodies on a quartz crystal microbalance using plasma-polymerized films for immunosensors," *Anal. Chem.* **68**, 1695–1700 (1996).

75. C. M. Duan and M. E. Meyerhoff, "Separation-free sandwich enzyme immunoassays using microporous gold electrodes and self-assembled monolayer/immobilized capture antibodies," *Anal. Chem.* **66**, 1369–1377 (1994).

76. J. P. Gosling, "A decade of development in immunoassay methodology," *Clin. Chem.* **36**, 1408–1427 (1990).

77. E. Ishikawa, S. Hashida, T. Kohno, and K. Hirota, "Ultrasensitive enzyme immunoassay," *Clin. Chim. Acta* **194**, 51–72 (1990).

78. W. C. W. Chan and S. M. Nie, "Quantum dot bioconjugates for ultrasensitive nonisotopic detection," *Science* **281**, 2016–2018 (1998).

79. M. B. M. Moronne, Jr., P. Gin, S. Weiss, and A. P. Alivisatos, "Semiconductor nanocrystals as fluorescent biological labels," *Science* **281**, 2013–2016 (1998).

80. S. D. Mangru and D. J. Harrison, "Chemiluminescence detection in intergrated post-separation reactors for microchip-based capillary electrophoresis and affinity electrophoresis," *Electrophoresis* **19**, 2301–2307 (1998).

81. X. Z. Wu, M. Suzuki, T. Sawada, and T. Kitamori, "Chemiluminescence on a microchip," *Anal. Sci.* **16**, 231–323 (2000).

82. M. Hashimoto, K. Tsukagoshi, R. Nakajima, K. Kondo, and A. Arai, "Microchip capillary electrophoresis using on-line chemiluminescence detection," *J. Chromatogr. A* **867**, 271–279 (2000).

83. J. Yakovleva, R. Davidsson, A. Lobanova, M. Bengtsson, S. Eremin, T. Laurell, and J. Emnéus, "Microfluidic enzyme immunoassay using silicon microchip with immobilized antibodies and chemiluminescence detection," *Anal. Chem.* **74**, 2994–3004 (2002).

84. C. A. Mirkin, R. L. Letsinger, R. C. Mucic, and J. J. Storhoff, "A DNA-based method for rationally organizing nanoparticles into macroscopic materials," *Nature (London)* **382**, 607–609 (1996).

85. A. P. Alivisatos, K. P. Johnsson, X. Peng, T. E. Wilson, C. J. Loweth,

M. B. Bruchez Jr., and P. G. Schultz, "Organization of 'nanocrystal molecules' using DNA," *Nature (London)* **382**, 609–611 (1996).

86. R. Elghanian, J. J. Storhoff, R. C. Mucic, R. L. Letsinger, and C. A. Mirkin, "Selective colorimetric detection of polynucleotides based on the distance-dependent optical properties of gold nanoparticles," *Science* **277**, 1078–1081 (1997).

87. C. J. Loweth, W. Caldwell, X. Peng, A. P. Alivisatos, and P. G. Schultz, "DNA-based assembly of gold nanocrystals," *Angew. Chem., Int. Ed.* **38**, 1808–1812 (1999).

88. N. T. K. Thanh and Z. Rosenaweig, "Development of an aggregation-based immunoassay for anti-protein a using gold manoparticles," *Anal. Chem.* **74**, 1624–1628 (2002).

89. N. Levit-Binnun, A. B. Lindner, O. Zik, Z. Eshhar, and E. Moses, "Quantitative detection of protein arrays," *Anal. Chem.* **75**, 1436–1441 (2003).

90. Z. F. Ma and S. Sui, "Naked-eye sensitive detection of immunoglubulin G by enlargement of Au nanoparticles *in vitro*," *Angew. Chem., Int. Ed.* **41**, 2176–2179 (2002).

91. N. Nath and A. Chilkoti, "A colorimetric gold nanoparticle sensor to interrogate biomolecular interactions in real time on a surface," *Anal. Chem.* **74**, 504–509 (2002).

92. B. S. Mann, W. Shenton, M. Li, S. Connolly, and D. Fitzmaurice, "Biologically programmed nanoparticle assembly," *Adv. Mater. (Weinheim, Ger.)* **12**, 147–150 (2000).

93. J. Nam, C. S. Thaxton, and C. A. Mirkin, "Nanoparticle-based bio-bar codes for the ultrasensitive detection of proteins," *Science* **301**, 1884–1886 (2003).

94. J. Masai, T. Sorin, and S. Kondo, "Scanning tunneling microscopic immunoassay: A preliminary experiment," *J. Vac. Sci. Technol. A* **8**, 713–717 (1990).

95. X. H. Ji, S. P. Xu, L. Y. Wang, M. Liu, K. Pan, H. Yuan, L. Ma, Y. B. Bai, and T. J. Li, "Immunoassay using the probe-labeled Au@Ag core-shell nanoparticles via surface-enhance Raman scattering," *Colloids and Surfaces A* **257−258**, 171–175 (2005).

96. A. T. Tu, "Peptide backbone conformation and microenvironment of protein side chains," in *Spectroscopy of Biological Systems*, R. J. H. Clark and R. E. Hester, Eds., Chap. 2, pp. 47–112, Wiley, Chichester (1986).

97. I. Harada and T. Takeuchi, "Raman and ultraviolet resonance Raman spectra of proteins and related compounds," in *Spectroscopy of Biological Systems*, Chap. 3, pp. 113–175, Wiley, Chichester (1986).

98. T. M. Cotton, J. M. Kim, and G. D. Chumanov, "Application of surface-enhanced Raman spectroscopy to biological systems," *J. Raman Spectrosc.* **22**, 729–742 (1991).

99. A. M. Ahern and R. L. Garrell, "Protein-metal interactions in protein-colloid conjugates probed by surface-enhanced Raman spectroscopy," *Langmuir* **7**, 254–261 (1991).

100. E. S. Grabbe and R. P. Buck, "Evidence for a conformational change with potential of adsorbed anti-IgG alkaline phosphatase conjugate at the silver electrode interface using SERS," *J. Electroanal. Chem.* **308**, 227–237 (1991).

101. P. C. Painter and J. L. Koenig, "Raman spectroscopic study of the structure of antibodies," *Biopolymers* **14**, 457–468 (1975).

102. M. Pezolet, M. Pigeon-Gosselin, and L. Coulombe, "Laser Raman investigation of the conformation of human immunoglobulin G," *Biochim. Biophys. Acta* **455**, 502–512 (1976).

103. W. Q. Xu, S. P. Xu, X. H. Ji, B. Song, and Y. B. Bai, "Preparation of gold colloid monolayer by immunological identification," *Colloids and Surfaces B* **40**, 169–172 (2005).

104. A. Michota and J. Bukowska, "Surface-enhanced Raman scattering (SERS) of 4-mercaptobenzoic acid on silver and gold substrates," *J. Raman Spectrosc.* **34**, 21–25 (2003).

105. T. Itoh, K. Hashimoto, and Y. Ozaki, "Polarization dependences of surface plasmon bands and surface-enhanced Raman bands of single Ag nanoparticles," *Appl. Phys. Lett.* **83**, 2274–2276 (2003).

106. X. H. Ji, L. Y. Wang, X. T. Zhang, Y. B. Bai, T. J. Li, Z. Z. Zhi, X. G. Kong, and Y. C. Liu, "Preparation of Au/Ag core-shell nanoparticles and its surface-enhanced Raman scattering effect," *Chem. J. Chinese Universities* **23**, 2357–2359 (2002).